Redox Biology 25 (2019) 101196

Contents lists available at ScienceDirect

Redox Biology

journal homepage: www.elsevier.com/locate/redox

Advanced oxidation protein products induce G1 phase arrest in intestinal epithelial cells via a RAGE/CD36-JNK-p27kip1 mediated pathway

Jie Shi[a], Shibo Sun[b], Yan Liao[a], Jing Tang[c], Xiaoping Xu[d], Biyan Qin[a], Caolitao Qin[a], Lishan Peng[e], Mengshi Luo[e], Lan Bai[a,*,1], Fang Xie[a,*,1]

[a] Guangdong Provincial Key Laboratory of Gastroenterology, Department of Gastroenterology, Nanfang Hospital, Southern Medical University, Guangzhou, Guangdong, 510515, China
[b] Department of Hepatobiliary Surgery, Nanfang Hospital, Southern Medical University, Guangzhou, Guangdong, 510515, China
[c] Department of Gastroenterology, The First Affiliated Hospital of Guangxi Medical University, Nanning, Guangxi, 530021, China
[d] Department of Gastroenterology, Hunan Provincial People's Hospital, Changsha, Hunan, 410005, China
[e] Southern Medical University, Guangzhou, Guangdong, 510515, China

ARTICLE INFO

Keywords:
Advanced oxidation protein products
G1 phase arrest
p27kip1
Cyclin E
Cyclin-dependent kinase 2

ABSTRACT

Intestinal epithelial cell (IEC) cycle arrest has recently been found to be involved in the pathogenesis of Crohn's disease (CD). However, the mechanism underlying the regulation of this form of cell cycle arrest, remains unclear. Here, we investigated the roles that advanced oxidation protein products (AOPPs) may play in regulating IEC cycle arrest. Plasma AOPPs levels and IEC cycle distributions were evaluated in 12 patients with CD. Molecular changes in various cyclins, cyclin-dependent kinases (CDKs), and other regulatory molecules were examined in cultured immortalized rat intestinal epithelial (IEC-6) cells after treatment with AOPPs. The *in vivo* effects exerted by AOPPs were evaluated using a normal C57BL/6 mouse model with an acute AOPPs challenge. Interestingly, plasma AOPPs levels were elevated in active CD patients and correlated with IEC G1 phase arrest. In addition, IEC treatment with AOPPs markedly reduced the expression of cyclin E and CDK2, thus sensitizing epithelial cells to cell cycle arrest both *in vitro* and *in vivo*. Importantly, we found that AOPPs induced IEC G1 phase arrest by modulating two membrane receptors, RAGE and CD36. Furthermore, phosphorylation of c-jun N-terminal kinase (JNK) and the expression of p27kip1 in AOPPs-treated cells were subsequently increased and thus affected cell cycle progression. Our findings reveal that AOPPs influence IEC cycle progression by reducing cyclin E and CDK2 expression through RAGE/CD36-depedent JNK/p27kip1 signaling. Consequently, AOPPs may represent a potential therapeutic molecule. Targeting AOPPs may offer a novel approach to managing CD.

1. Introduction

Crohn's disease (CD) is a relapsing inflammatory disease of the gastrointestinal tract [1]. Throughout the pathogenesis of CD, intestinal epithelial cells (IEC) remain the main targets of various pro-inflammatory factors [2,3]. IEC dysfunction has been reported to result in increased intestinal permeability and excessive translocation of commensal bacteria into the lamina propria, thus contributing to chronic mucosal inflammation in CD [4,5]. IEC cycle arrest, and cell death, are hallmarks of intestinal mucosal inflammation and have been recognized as both initiating and aggravating factors in the pathogenesis of CD [6,7]. However, the regulation of epithelial cell cycle arrest remains poorly understood.

Cell cycle arrest is a complex process, often triggered by various stimuli in a variety of pathophysiological conditions [8,9]. In recent studies, oxidative stress has been verified as one of the stimuli that induces cell cycle arrest in the setting of various disease processes [10,11]. Advanced oxidation protein products (AOPPs), novel protein markers of oxidant-mediated protein damage, have been found to participate in a variety of pathological changes, including the induction of cell death [12], endothelial cell perturbation [13], and the formation of atherosclerosis [14]. Importantly, the accumulation of AOPPs has been reported to contribute substantially to cell cycle arrest [15]. Our previous study confirmed that AOPPs induce S-phase arrest in hepatocytes and thus impair liver regeneration [16].

Recent studies have highlighted important roles for cyclin-dependent kinase inhibitors (CKIs) in regulating the epithelial cell cycle during inflammation [17]. The overexpression of CKIs, which regulate

* Corresponding authors.
E-mail addresses: bailan99@hotmail.com (L. Bai), stellaff@126.com (F. Xie).
[1] These authors contributed equally to this work.

https://doi.org/10.1016/j.redox.2019.101196
Received 8 November 2018; Received in revised form 28 February 2019; Accepted 8 April 2019
Available online 17 April 2019

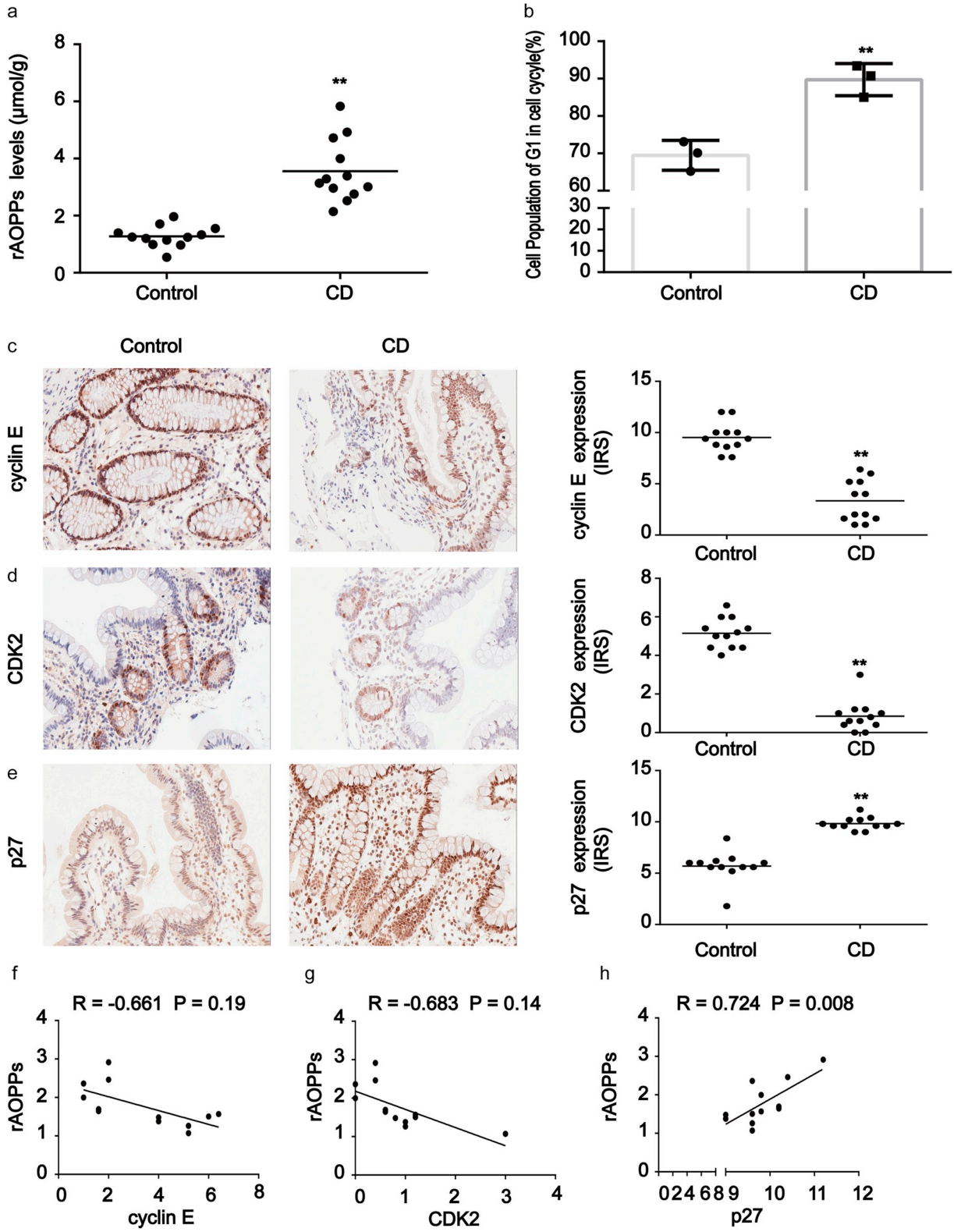

Fig. 1. Accumulation of AOPPs in plasma correlated with cell cycle arrest in CD patients. (a) The relative plasma concentration of rAOPPs in controls (n = 12) and CD patients (n = 12). Plasma AOPPs were increased in CD patients compared to healthy subjects. (b) Bar graphs representing flow cytometry results showing G1 phase arrest in CD patients (n = 3) when compared with healthy controls (n = 3). (c–e) Images representative of immunohistochemical staining revealed the expression of cyclin E, CDK2 and p27kip1 in intestinal tissues from 12 healthy subjects and 12 CD patients. Scale bar, 20 μm. Data for the accompanying graphs were generated from immunoreactive scores (IRS). Overall, these results show a reduction of cyclin E (c) and CDK2 (d) with an induction in p27kip1 (e). Data are represented as IRS of cyclin E, CDK2 and p27kip1 in controls and CD patients. (f, g) Pearson correlation and linear analysis showing that the accumulation of AOPPs was negatively associated with cyclin E and CDK2 expression in tissues from CD patients (R = −0.661, P = 0.19; R = −0.683, P = 0.14). (h) Pearson correlation and linear analysis showing that the increased expression of p27kip1 was positively associated with AOPPs levels (R = 0.724, P = 0.008). **P < 0.01 *versus* controls. CD, Crohn's disease; rAOPPs, relative AOPPs.

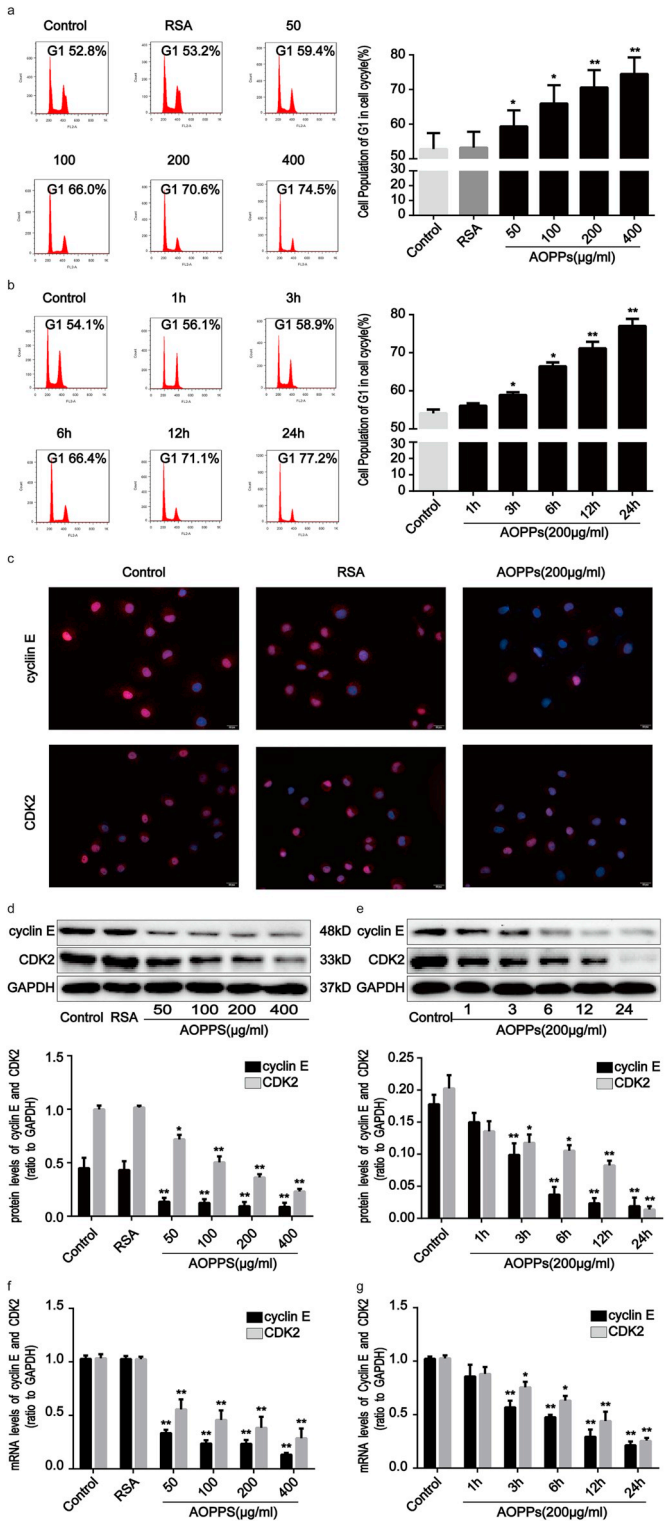

Fig. 2. AOPPs treatment induced G1 phase arrest in IEC-6 cells in a concentration- and time-dependent manner. IEC-6 cells were treated with control medium, RSA (50 μg/ml), or the indicated concentration of AOPPs for 24 h (a, d, f) or 200 μg/ml of AOPPs at the indicated times (b, e, g), or 200 μg/ml of AOPPs for 24 h (c). Cell cycle distributions were determined by quantitative fluorescence-activated cell sorting (FACS) (a, b). Flow cytometry revealed that a challenge with AOPPs increased the percentage of cells arrested in G1 in a dose- and time-dependent manner. Quantitative analyses of FACS data represent the percentage of G1 phase cells. (c) Immunofluorescence staining for cyclin E and CDK2 revealed that stimulation with AOPPs resulted in a significant reduction of cyclin E and CDK2 in IEC-6 cells. Scale bar, 20 μm. (d, e) Representative Western blotting and bar graphs depicting densitometry quantification showing a reduction of cyclin E and CDK2 protein expression in IEC-6 cells after AOPPs treatment. (f, g) mRNA expression of cyclin E and CDK2 was determined by qPCR. Bar graphs showing qPCR results revealed that AOPPs treatment reduced cyclin E and CDK2 gene expression. Relative protein and mRNA levels of cyclin E and CDK2 were normalized with GAPDH, respectively. Data are presented as mean ± SD from three independent experiments; error bars indicate SD. *P < 0.05 and **P < 0.01 *vs* control. GAPDH, glyceraldehyde-3-phosphate dehydrogenase; qPCR, quantitative real-time polymerase chain reaction.

the cell cycle by binding to and inactivating a number of cyclin-CDK complexes, results in IEC cycle arrest [18]. One member of the CKI family, p27kip1, is well known to be a negative regulator of G1 progression [19]. AOPPs were previously reported to induce the over-expression of p27kip1 and cause G1 phase arrest in human proximal tubular cells [15]. However, the epithelial cell activity of p27kip1 in the setting of chronic inflammatory conditions, such as CD, has not been studied extensively.

Our previous studies found plasma AOPPs to be elevated in CD patients and deposited in intestinal tissues; AOPPs accumulation resulted in IEC depletion and promoted epithelial-mesenchymal transition (EMT) via NADPH oxidase activation and the generation of reactive oxygen species (ROS) [20,21]. In addition, AOPPs reduced the expression of calcium transport channels in the intestinal epithelium, resulting in inflammatory bowel disease-associated osteoporosis [22]. These findings led us to address the question of whether AOPPs induce IEC cycle arrest, thereby initiating and exacerbating inflammatory injury. In the present study, our findings reveal that AOPPs exhibit their negative regulatory function upon IEC cycle progression by activating the RAGE/CD36-c-jun N-terminal kinase (JNK)-p27kip1 signaling pathway, thus implicating AOPPs as key players in the pathogenesis of CD.

2. Results

2.1. Plasma AOPPs accumulate in active CD and correlate with IEC G1 phase arrest

To investigate the potential role of AOPPs in IEC cycle arrest, we evaluated the plasma AOPPs concentrations of 12 active CD patients and 12 healthy subjects. Flow cytometry was used to measure the cell cycle distribution of IEC in surgically resected tissues. In comparison with healthy subjects, plasma AOPPs levels were increased in active CD patients ($p < 0.01$; Fig. 1a). In addition, intestinal epithelial cell G1 phase arrest was quite marked in CD patients ($p < 0.01$; Fig. 1b). To further clarify the relationship between AOPPs and the IEC cycle, we evaluated the expression of G1 phase-associated proteins and cyclin-dependent kinases (CDK) including cyclin E, cyclin D, CDK2, CDK4, and CDK6 in intestinal tissues. As shown in Fig. 1c and d, staining revealed high concentrations of cyclin E and CDK2 in normal tissues while revealing low concentrations in CD-affected tissues. Staining for cyclin D, CDK4, and CDK6 did not differ significantly between the two tissue groups (data not shown). Immunoreactive score analysis further revealed that the intensities of cyclin E and CDK2 in CD tissues were weaker than in normal tissues ($p < 0.01$). In contrast, CD tissues showed significantly stronger p27kip1 staining than tissues from healthy subjects ($p < 0.01$; Fig. 1e). Pearson correlation and linear regression analyses additionally revealed that AOPPs accumulation was negatively correlated with cyclin E and CDK2 expression in CD tissues (Fig. 1f and g), while high expression of p27kip1 was strongly and positively correlated with increased AOPPs levels ($R = 0.724$, $p = 0.008$; Fig. 1h). These findings suggested that the accumulation of AOPPs was associated with IEC G1 phase arrest in CD patients.

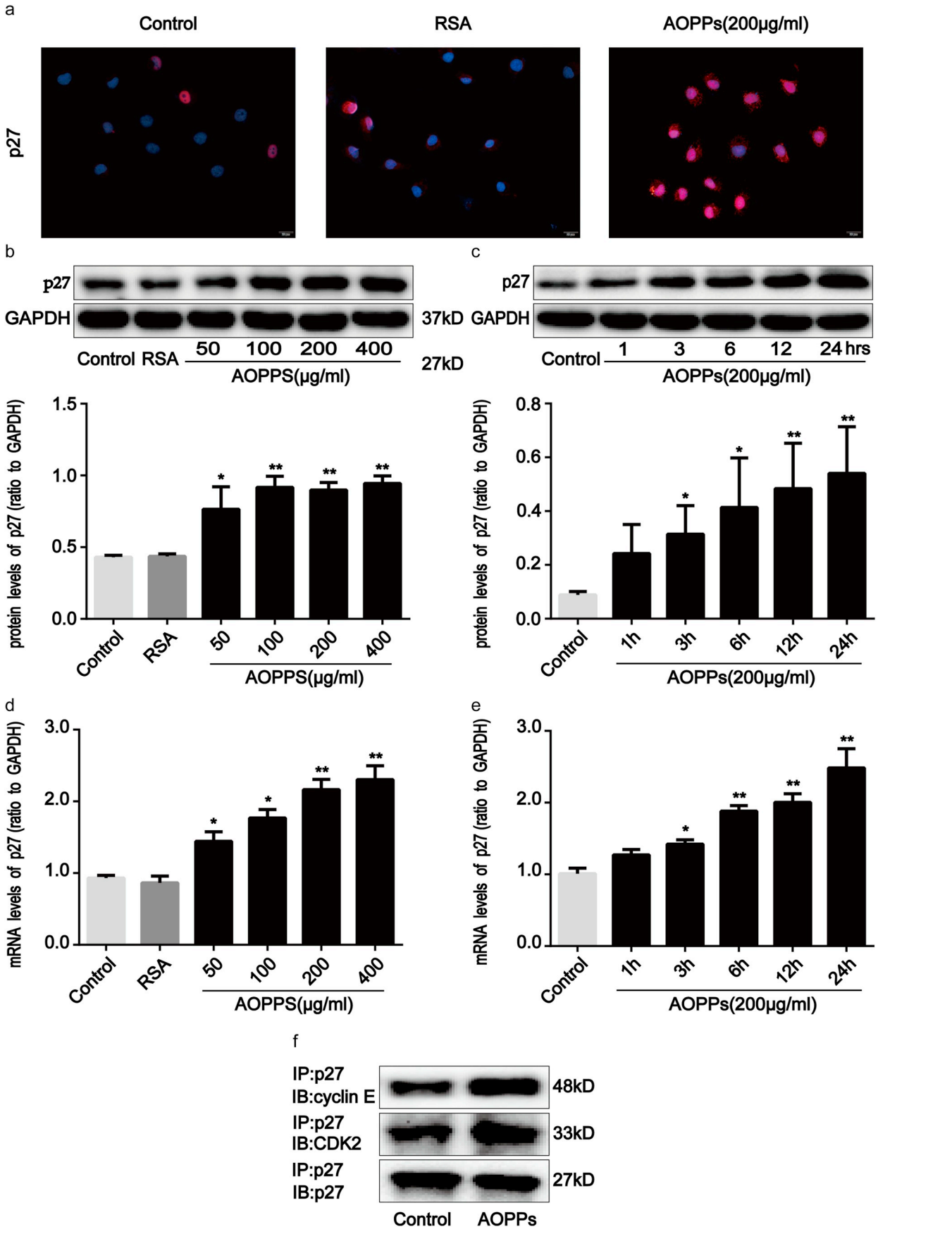

(caption on next page)

Fig. 3. AOPPs-enhanced p27kip1 expression in IEC-6 cells. IEC-6 cells were treated with control medium, RSA (50 μg/ml), or 200 μg/ml of AOPPs for 24 h (a, f), or the indicated concentration of AOPPs for 24 h (b, d) or 200 μg/ml of AOPPs for the indicated times (c, e). (a) Immunofluorescence staining for p27kip1 revealed that AOPPs stimulation enhanced the expression of p27kip1 in IEC-6 cells. Scale bar, 20 μm. (b, c) Representative Western blotting and bar graphs depicting densitometry quantification and showing augmentation of p27kip1 in IEC-6 cells after AOPPs treatment. (d, e) mRNA expression of p27kip1 was determined by qPCR. Bar graphs showing qPCR results revealed that AOPPs treatment increased p27kip1 gene expression in a dose- and time-dependent manner. Relative protein and mRNA levels were normalized with GAPDH, respectively. (f) Results of co-immunoprecipitation analysis revealed that AOPPs treatment enhanced the binding of p27kip1 to cyclin E-CDK2 complexes in IEC-6 cells. Data are presented as mean ± SD from three independent experiments; error bars indicate SD. *P < 0.05 and **P < 0.01 versus control.

2.2. AOPPs induce G1 phase arrest in IEC-6 cells

Based on the findings mentioned above, we next used normal rat IEC-6 cells as an *in vitro* model to investigate whether the accumulation of AOPPs directly regulates the IEC cycle. We studied the cell cycle distribution of IEC-6 cells by quantitative fluorescence-activated cell sorting (FACS) analysis. Treatment of cells with AOPPs increased the proportion of IEC-6 cells arrested in G1 phase in a concentration- and time-dependent manner (Fig. 2a and b). We further studied the expression of cyclins and CDK proteins related to G1 phase arrest using immunofluorescence, Western blotting, and quantitative real-time polymerase chain reaction (RT-qPCR) analyses. Immunofluorescence confirmed that treatment with AOPPs significantly reduced cyclin E and CDK2 expression (Fig. 2c). Similarly, exposure of IEC-6 cells to AOPPs led to the downregulation of cyclin E and CDK2 expression at both protein (Fig. 2d and e) and gene (Fig. 2g and h) levels. Cyclin D, CDK4, and CDK6 expression was unaffected by AOPPs treatment (Supplementary Fig. 1a and b). We thus concluded that AOPPs act to promote G1 phase arrest via cyclin E and CDK2 suppression in IEC-6 cells.

2.3. AOPPs induce G1 phase arrest in IEC-6 cells via p27kip1 regulation

p27kip1 is a critical modulator of G1 progression and interacts with and inhibits a number of cyclin-CDK complexes [19]. We studied p27kip1 levels and the interaction of p27kip1 with cyclin-CDK complexes in AOPPs-treated IEC-6 cells. As shown in Fig. 3a–e, AOPPs treatment significantly induced dose- and time-dependent increases in p27kip1, while unmodified RSA had no such effect. Fig. 3f shows how the incubation of IEC-6 cells with AOPPs induced more binding of p27kip1 to cyclin E-CDK2 complexes when compared with cells cultured in control medium, whereas the combination of p27kip1 with cyclin D-CDK4/6 complexes did not increase (Supplementary Fig. 1c). To evaluate whether the expression of p27kip1 is required for AOPPs to suppress cell cycle progression in IEC-6 cells, we silenced p27kip1 using small interfering RNA (siRNA) transfection before exposing cells to AOPPs. The silencing efficiency was then verified by Western blotting. The transfection of siRNA resulted in a 73% reduction of protein expression (Supplementary Fig. 2a). As expected, p27kip1 siRNA transfection significantly alleviated AOPPs-induced G1 phase arrest ($p < 0.01$; Fig. 4a), the inhibition of cyclin E and CDK2 (Fig. 4b–d), as well as the interaction of p27kip1 with cyclin E-CDK2 complexes in IEC-6 cells (Fig. 4e). These results suggested that p27kip1 plays a critical role in AOPPs-induced G1 phase arrest in IEC-6 cells.

2.4. AOPPs induce G1 phase arrest in IEC-6 cells via the activation of JNK

Previous research has demonstrated that the activation of intracellular mitogen-associated protein kinases (MAPKs), including JNK, extracellular signal-regulating kinases 1/2 (ERK1/2 or p44/42 MAPK), and p38 MAPK, regulates cellular responses to stress and affects cell growth and death processes [23]. To determine whether the MAPK pathway is involved in AOPPs-induced G1 phase arrest, we evaluated MAPK activity in IEC-6 cell cultures treated with AOPPs. Our findings revealed that JNK (Fig. 5a), ERK1/2 and p38 MAPK (Supplementary Fig. 3a) phosphorylation markedly increased from 30 to 120 min after AOPPs treatment ($p < 0.01$). To further evaluate the role of the MAPK pathway in G1 phase arrest, IEC-6 cell cultures were incubated with a JNK inhibitor (SP600125), a MEK1/2 inhibitor (U0126) and a p38 MAPK inhibitor (SB203580), respectively, prior to AOPPs treatment. Our findings revealed that the AOPPs-induced G1 phase arrest in IEC-6 cells was ameliorated by the JNK inhibitor ($p < 0.01$; Fig. 5b), but not by MEK1/2 and p38 MAPK inhibitors (Supplementary Fig. 3b). We subsequently confirmed that the JNK inhibitor restored AOPPs-induced expression changes in cyclin E, CDK2, and p27kip1 (Fig. 5c–e). In addition, the increased binding of p27kip1 to cyclin E-CDK2 complexes in AOPPs-treated IEC-6 cells was attenuated by the JNK inhibitor (Fig. 5f), suggesting that the AOPPs-induced G1 phase arrest in IEC-6 cells is mediated by JNK activation.

2.5. AOPPs enhance the expression of RAGE and CD36 in IEC-6 cells

It has previously been reported that cell membrane receptors, including RAGE and CD36, are involved in a variety of intestinal inflammatory responses [24–26]. RAGE and CD36 are also known to be responsible for AOPPs-triggered cellular responses to oxidative stress [13,27,28]. As shown in Fig. 6a, AOPPs enhanced the expression of RAGE and CD36 in IEC-6 cells. Moreover, AOPPs challenge significantly augmented RAGE and CD36 expression in cultured IEC-6 cells at both the protein and mRNA levels in a dose- and time-dependent manner (Fig. 6b–i). We further evaluated whether AOPPs interact with RAGE or CD36 in IEC-6 cells by using a co-immunoprecipitation assay. Fig. 6j and k show that AOPPs were detected by an anti-AOPPs antibody in anti-RAGE and anti-CD36 immunoprecipitates from AOPPs-treated cells, but not in control cells. These findings therefore revealed that AOPPs increase the expression of RAGE and CD36, as well as the interaction of AOPPs with these two membrane receptors.

2.6. The AOPPs-induced G1 phase arrest in IEC-6 cells is mediated by RAGE and CD36

To confirm the role of RAGE and CD36 in AOPPs-induced IEC-6 G1 phase arrest, we pre-incubated cells with RAGE- and CD36-specific siRNA respectively prior to AOPPs exposure. The efficiency of each siRNA was demonstrated by Western blotting. Transfection of siRNA resulted in a ~71.5% and ~72.0% reduction of protein expression, respectively (Supplementary Fig. 2b). As shown in Fig. 7a, both siRNAs significantly inhibited AOPPs-induced G1 phase arrest ($p < 0.01$). Similarly, the AOPPs-induced activation of JNK was clearly inhibited by RAGE and CD36 siRNA ($p < 0.01$; Fig. 7b). Furthermore, knocking down endogenous RAGE and CD36 expression restored the AOPPs-induced reduction of cyclin E and CDK2 and overexpression of p27kip1 (Fig. 7c and d), as well as the interaction of p27kip1 with cyclin E-CDK2 complexes (Fig. 7e). These findings confirm that RAGE and CD36 are crucial mediators of AOPPs-induced IEC-6 G1 phase arrest.

2.7. Effects of an acute AOPPs challenge upon IEC G1 phase arrest in mice

To examine whether the effects we observed *in vitro* also occur *in vivo*, we treated normal male C57BL/6 mice with a daily intraperitoneal injection containing AOPPs for 5 days. Flow cytometry analysis revealed primary IEC G1 phase arrest to be significantly increased in

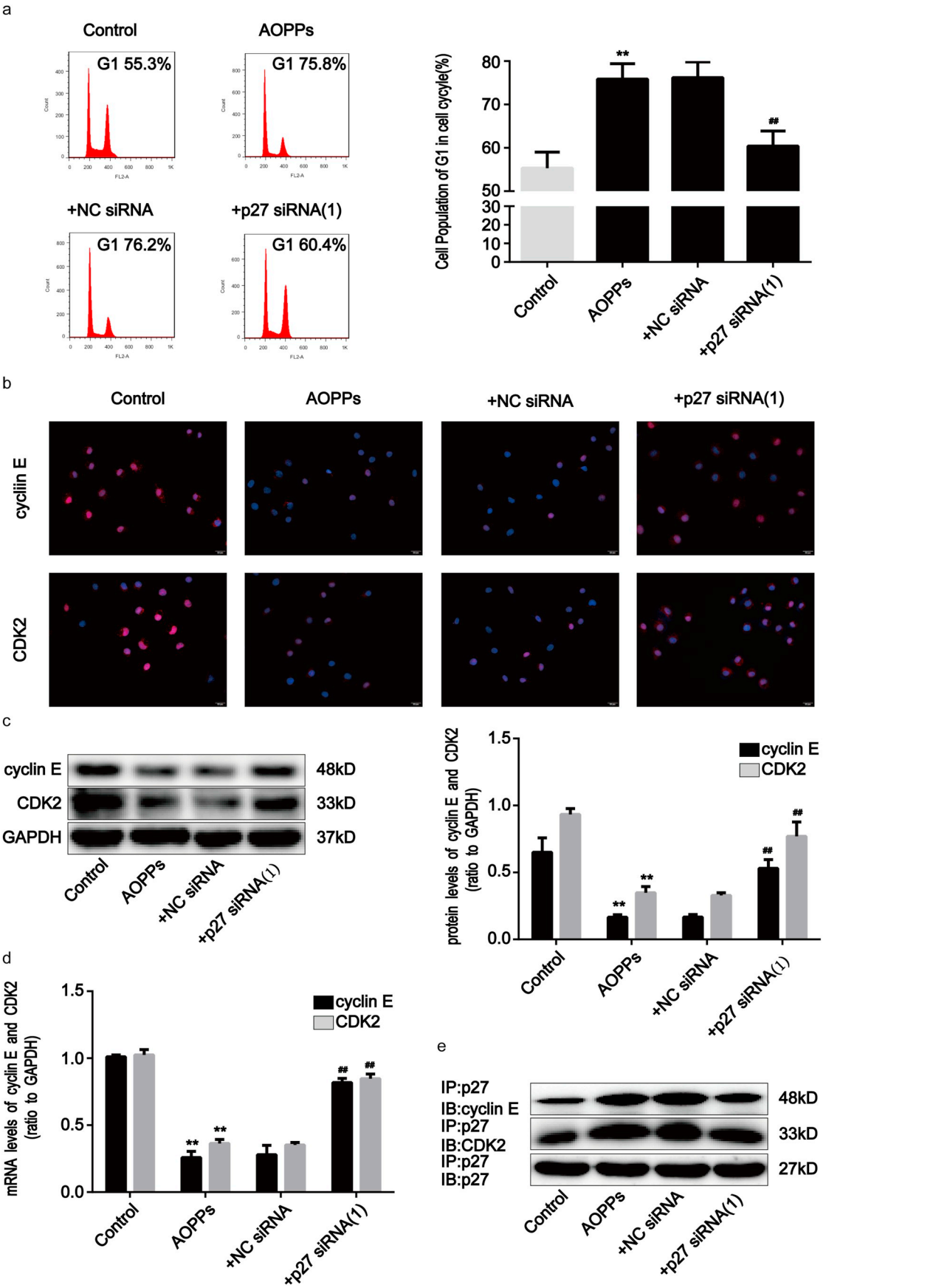

(caption on next page)

Fig. 4. AOPPs-induced G1 phase arrest in IEC-6 cells via p27kip1 regulation. IEC-6 cells were transfected with p27kip1 siRNA for 48 h and then incubated with 200 μg/ml of AOPPs for 24 h. (a) Flow cytometry results revealed that p27kip1 siRNA attenuated the effects of AOPPs-induced G1 phase arrest in IEC-6 cells. Quantitative analyses of FACS data represent G1 phase cell percentages. (b) Immunofluorescence staining for cyclin E and CDK2 revealed that p27kip1 siRNA enhanced the expression of cyclin E and CDK2 in AOPPs-treated cells. Scale bar, 20 μm. (c) Representative Western blotting and bar graphs depicting densitometry quantification and showing that AOPPs-induced reduction of cyclin E and CDK2 protein expression were reversed by p27kip1 siRNA transfection. (d) Bar graph representing qPCR results illustrating that p27kip1 siRNA enhanced cyclin E and CDK2 mRNA expression in AOPPs-treated cells. Relative protein and mRNA levels were normalized with GAPDH, respectively. (e) Results of co-immunoprecipitation analysis showing that p27kip1 siRNA transfection significantly alleviated AOPPs-induced interaction of p27kip1 with cyclin E-CDK2 complexes in IEC-6 cells. Data are presented as mean ± SD from three independent experiments; error bars indicate SD. *P < 0.05 and **P < 0.01 *vs* control; #P < 0.05 and ##P < 0.01 *versus* AOPPs-treated cells. siRNA, small interfering RNA; NC siRNA, Negative Control siRNA; + NC siRNA, AOPPs plus NC siRNA treatment; +p27 siRNA (1), AOPPs plus p27 siRNA (1) treatment.

AOPPs-treated mice when compared with mice administered with a vehicle (phosphate-buffered saline [PBS]) ($p < 0.01$; Fig. 8a). As illustrated in Fig. 8b and c, the expression of cyclin E and CDK2, at both the mRNA and protein levels, was reduced after AOPPs treatment in mice ($p < 0.01$). Immunohistochemistry further confirmed weakly positive staining of cyclin E and CDK2 in AOPPs-challenged mice (Fig. 8d). These data suggest that AOPPs trigger IEC G1 phase arrest *in vivo*.

2.8. AOPPs induce IEC G1 phase arrest in mice via the RAGE/CD36-JNK-p27kip1 pathway

Finally, we investigated the effects of AOPPs upon activation of the RAGE/CD36-JNK-p27kip1 pathway in mice. Compared with vehicle-treated mice, RAGE and CD36 expression, activation of JNK, p27kip1 expression, and binding of p27kip1 to cyclin E-CDK2 complexes, were significantly enhanced in AOPPs-challenged mice (Fig. 9a–h). To further clarify the role of the RAGE/CD36-JNK-p27kip1 pathway in AOPPs-induced IEC G1 phase arrest *in vivo*, we treated mice with AOPPs in addition to RAGE, CD36, and p27kip1 siRNA, respectively. The efficiency of each siRNA was confirmed by Western blotting. Transfection of siRNA resulted in a marked reduction of protein expression (Supplementary Fig. S4). As shown in Fig. 8a–d, the knock-down of RAGE, CD36, and p27kip1 attenuated AOPPs-induced primary IEC G1 phase arrest and the inhibition of cyclin E and CDK2 in mice. We also found that the blockade of RAGE and CD36 significantly reversed the AOPPs-induced activation of JNK and the overexpression of p27kip1, as well as the interaction of p27kip1 with cyclin E-CDK2 complexes (Fig. 9d–h). Collectively, these results indicate that AOPPs induce *in vivo* IEC G1 phase arrest in a RAGE/CD36-JNK-p27kip1-dependent manner.

3. Discussion

The etiology of CD is associated with excessive mucosal damage caused by specific intestinal antigens, as well as chronic mucosal inflammation caused by commensal bacterial translocation into the lamina propria through impairments in the intestinal mucosa [29,30]. Intestinal healing after inflammatory attacks is important in the maintenance and recovery of intestinal mucosal integrity and intestinal homeostasis [31,32]. IEC are the structural and functional base of the intestinal mucosal barrier, and their cycle arrest and death are implicated in both the initiation and progression of CD due to homeostatic dysregulation [7,33]. We previously found that cell death plays a crucial role in the pathogenesis of CD via a redox pathway. However, the fundamental mechanisms of cell cycle arrest in IEC have not yet been elucidated. Here, we found marked G1 phase arrest in CD intestinal epithelium and determined that this correlated with the deposition of AOPPs. We also provided *in vivo* and *in vitro* evidence that AOPPs induced the occurrence of IEC G1-phase arrest via a RAGE/CD36-JNK-p27kip1 pathway.

Our previous study demonstrated that the accumulation of AOPPs induced excessive NADPH oxidase-dependent generation of intracellular superoxide, which in turn activated cascades of signaling events, triggered apoptosis, and resulted in EMT in IEC [20,21]. Despite the fact that cell apoptosis and EMT are the direct consequences of AOPPs treatment, how AOPPs transmit signals across the IEC plasma membrane to initiate specific transduction pathways remains poorly understood. Perhaps the primary reasons for this are that specific receptors for AOPPs are located on cell membranes. RAGE is a member of the immunoglobulin superfamily and has been implicated in the transduction of signals from multiple ligands, including advanced glycation end products (AGEs) and AOPPs [34,35]. RAGE has been found to play a key role in multiple epithelial dysfunctions via transport signals originating from the extracellular environment [36,37]. In this study, we provided several lines of evidence demonstrating that the AOPPs-induced IEC G1-phase arrest is mainly mediated by RAGE. Previous research also found that CD36, a transmembrane protein of the class B scavenger receptor, is capable of binding AOPPs [38]. CD36 serves as an important receptor in transmitting signals from AOPPs among various cell types, including cardiomyocytes and proximal tubular epithelial cells [12,35]. Here, we verified that the knock-down of CD36 partly attenuated AOPPs-induced IEC G1-phase arrest. To our knowledge, this is the first study to identify the interaction of AOPPs with RAGE and CD36 in IEC; our findings revealed that RAGE and CD36 receptors play crucial roles in AOPPs-mediated IEC G1-phase arrest.

MAPKs are important mediators playing a pivotal role in cellular differentiation, proliferation, and survival, including the JNK, extracellular signal-regulating kinase1/2 (ERK1/2 or p44/42 MAPK) and p38 MAPK [39–42]. In the present study, we found enhanced levels of JNK phosphorylation after treatment of IEC with AOPPs. Moreover, the membrane receptors RAGE and CD36 have also been identified to be upstream regulators of JNK signaling. Our findings were consistent with previous reports of RAGE and CD36-triggered JNK/MAPK phosphorylation in hepatocytes, cardiomyocytes and macrophages [43–46]. Moreover, JNK, but not ERK1/2 or p38 MAPK phosphorylation, has been identified to play a role in IEC AOPPs-triggered G1 phase arrest in this study, but whether there is a redox-dependent effect on JNK-mediated G1 phase arrest should be further investigated. In our previous study, AOPPs induced the impairment of liver regeneration via S-phase arrest in hepatocytes. In addition, we showed that AOPPs stimulation triggered JNK phosphorylation. Further investigation revealed that JNK signaling is not the key regulator in AOPPs-induced S-phase arrest in hepatocytes [16]. Our observations suggest that the effect of JNK phosphorylation in AOPPs-induced cell cycle arrest depend upon the particular cell line.

Control of G1 to S phase transition in the cell cycle is crucial for the regulation of cell proliferation [47]. Reports have shown that the expression of D-type cyclins and CDK4/6 activation occurs in early G1 phase [48]. However, it is not until near the end of G1, when cyclin E is expressed and Cdk2 is activated [49]. Our studies have shown that intracellular protein levels and kinase activities of the G1 phase, such as cyclin E and CDK2, were reduced in IEC after treatment with AOPPs, but cyclin D and CDK4/6 were not affected, thus suggesting disruption of late G1 phase. p27kip1, a member of the Cip/Kip family of CDK inhibitors, binds to a wide range of cyclin-CDK complexes, including cyclin D-CDK4/6 and cyclin E-CDK2, which are active throughout G1 and S phases [18]. The effects of AOPPs upon cell cycle machinery shows similarities with alterations observed during IFN-α-induced G1 phase arrest [50], including the upregulation of p27kip1 protein. AOPPs treatment, analogous to the effects of CRP and TGF-β

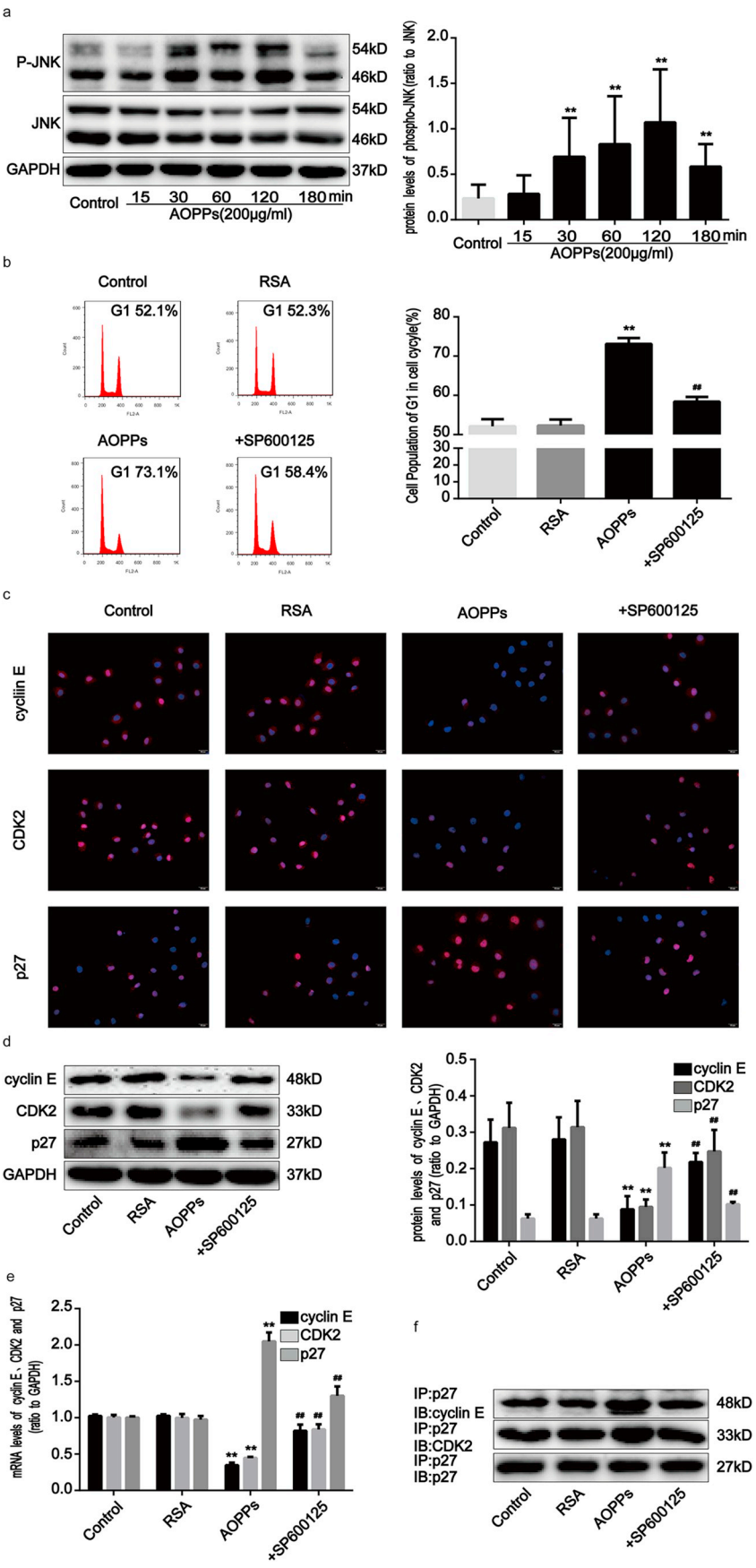

Fig. 5. AOPPs-induced G1 phase arrest in IEC-6 cells via the activation of JNK. IEC-6 cells were treated with 200 μg/ml of AOPPs for the time periods indicated (a) or pretreated with a JNK inhibitor (SP600125), at 10 μM, for 1 h and then incubated with 200 μg/ml of AOPPs for 24 h (b–e). (a) Representative Western blotting and densitometry quantification showing that AOPPs enhanced the phosphorylation of JNK in IEC-6 cells in a time-dependent manner. (b) Flow cytometry showing that the JNK inhibitor suppressed AOPPs-induced G1 phase arrest in IEC-6 cells. Quantitative analyses of FACS data represent G1 phase cell percentages. (c) Immunofluorescence staining for cyclin E, CDK2 and p27kip1 revealed that a JNK inhibitor enhanced the expression of cyclin E and CDK2 and weakened the expression of p27kip1 AOPPs-treated cells. Scale bar, 20 μm. (d) Representative Western blotting and bar graphs depicting densitometry quantification revealed that the AOPPs-induced reduction of cyclin E and CDK2 and upregulation of p27kip1 could all be blocked by a JNK inhibitor. (e) Bar graph showing the results of qPCR assays for mRNA expression. The JNK inhibitor increased cyclin E and CDK2 expression and decreased p27kip1 expression in IEC-6 cells after AOPPs treatment. Relative protein and mRNA levels were normalized with GAPDH, respectively. (f) Results of co-immunoprecipitation analysis showing that the JNK inhibitor attenuated the AOPPs-induced increased binding of p27kip1 to cyclin E-CDK2 complexes in IEC-6 cells. Data are presented as mean ± SD from three independent experiments; error bars indicate SD. *P < 0.05 and **P < 0.01 *versus* control; #P < 0.05 and ##P < 0.01 *versus* AOPPs-treated cells. JNK, c-jun N-terminal kinase. +SP600125, AOPPs plus an inhibitor of JNK treatment.

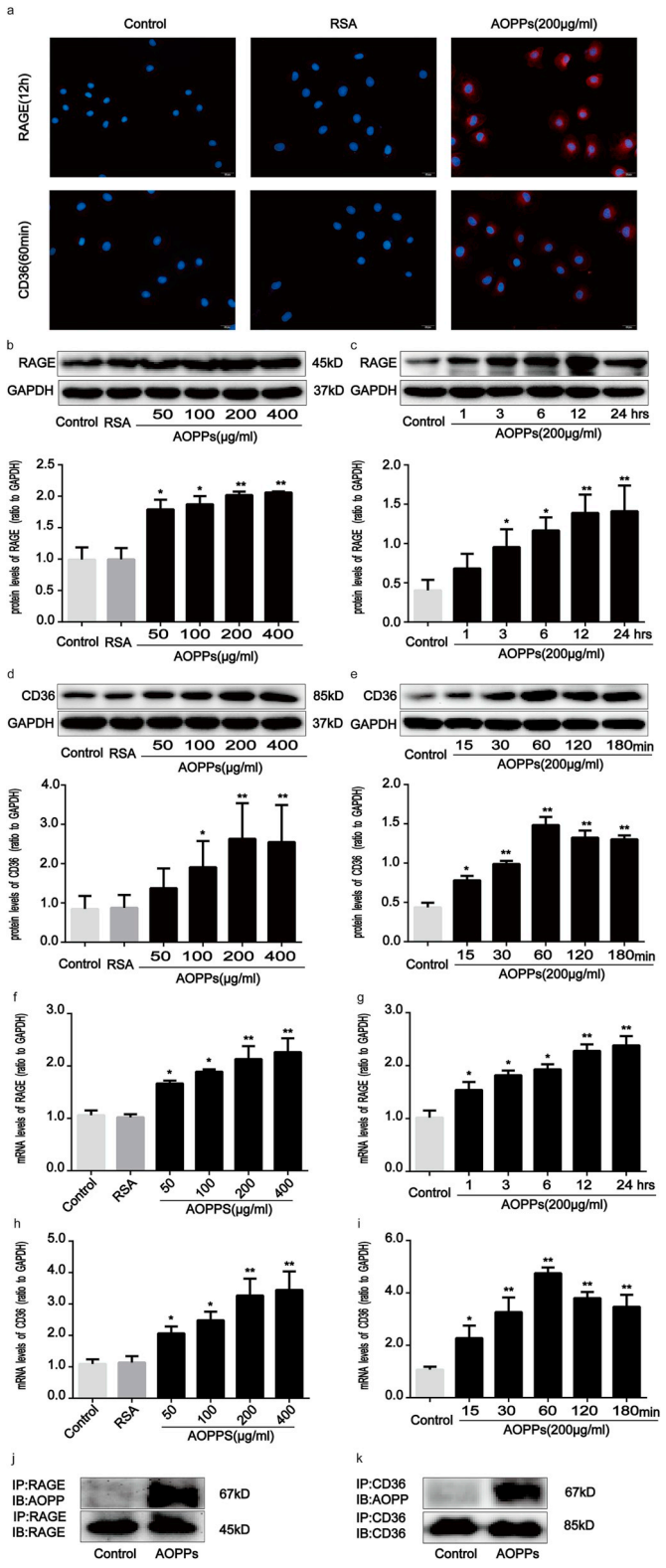

Fig. 6. AOPPs treatment enhanced RAGE and CD36 expression in IEC-6 cells. IEC-6 cells were incubated with 200 μg/ml of AOPPs for 12 h (a, j) or 60min (a, k), or the indicated concentrations of AOPPs for 12 h (b, f) or 60min (d, h), or 200 μg/ml of AOPPs for the time periods otherwise indicated (c, e, g, i). (a) Immunofluorescence staining for RAGE and CD36 revealed AOPPs stimulation to have resulted in a significant induction of RAGE and CD36 in the IEC-6 cell membrane. Scale bars, 20 μm. (b–i) Representative Western blotting and bar graphs representing mRNA levels and showing dose- and time-dependent effects of AOPPs treatment on upregulating RAGE and CD36 expression. Relative protein and mRNA levels were normalized with GAPDH, respectively. (j, k) Co-immunoprecipitation of AOPPs and RAGE or CD36 in cultured IEC-6 cells. The binding of AOPPs to RAGE or CD36 was analyzed by immunoprecipitation using anti-RAGE or anti-CD36 antibodies and was followed by immunoblotting using an anti-AOPPs antibody. Data are presented as mean ± SD from three independent experiments; error bars indicate SD. *P < 0.05 and **P < 0.01 *vs.* control. RAGE, receptor for advanced glycation end products; CD36, a scavenge receptor.

[19,51,52], resulted in the increased association of p27kip1 protein with cyclin E-CDK2 complexes, thereby inhibiting their activity. Despite recent studies having demonstrated that the elevation of p27kip1 directly inhibits the expression of cyclin D1 or the activity of cyclin D-CDK4 complexes [53,54], our current results revealed that AOPPs did not affect the combination of p27kip1 with cyclin D-CDK4/6 complexes. We propose that AOPPs induced IEC arrest late in the G1 phase via p27kip1.

In addition, we found that the AOPPs-induced upregulation of p27 kip1 was associated with upstream JNK phosphorylation in IEC-6 cells. Recent investigations have revealed that p27 kip1 is an important target gene for MAPK signaling pathways, including MAPK and MAPK kinase (MAPKK) [55–57]. Downstream of JNK, p27 kip1 expression was inhibited by a JNK inhibitor along with reversal of G1 phase arrest. Our current findings agree with previous research that JNK negatively regulate cell cycle progression from G1 to S phases in response to mammalian cell stress [58].

In summary, our findings reveal that AOPPs possess a potent ability to suppress cell cycle progression and DNA synthesis in IEC. This inhibition of cell cycle progression may contribute to the obstruction of self-healing in IEC. In addition, we provide mechanistic evidence that cell cycle arrest in IEC may be regulated through the enhanced expression of RAGE/CD36, phosphorylation of JNK, and activation of p27kip1 with subsequent inhibition of related cell cycle proteins such as cyclin E and CDK2. Thus, targeting AOPPs may present a novel and effective therapeutic strategy for the management of CD.

4. Materials and methods

4.1. Human tissues and blood samples

Intestinal specimens and blood samples were collected from 12 patients with CD. Three of these patients underwent surgical resection while the rest underwent endoscopy at Nanfang Hospital of Southern Medical University (Guangzhou, China) from 2014 to 2015. The clinical features of these patients are shown in Table 3. The diagnosis of CD was based on established clinical and histological criteria. Patients with malignant tumors, cardiovascular diseases, severe infections, or who were using infliximab were excluded from this study. Normal intestinal tissues, used as controls, were obtained from 12 healthy volunteers without any coexisting disease. Venous blood samples were collected prior to surgery or endoscopy. All procedures followed the ethical principles of the World Medical Association (WMA) Declaration of Helsinki. This study was approved by the Medical Ethical Committee of Nanfang hospital.

4.2. Plasma AOPPs determination

The concentration of AOPPs in plasma was assessed using spectrophotometry and expressed in equivalents of chloramine-T, as described previously[16]. In brief, 200 μl of serum samples (1:5 diluted in PBS), 200 μl of chloramine-T (Sigma) for calibration (0–100 μM), and 200 μl of PBS as a blank control, were placed in a 96-well plate. Subsequently, 10 μl of 1.16 M potassium iodide and 20 μl of acetic acid was added to each well, and absorbance at 340 nm was measured immediately.

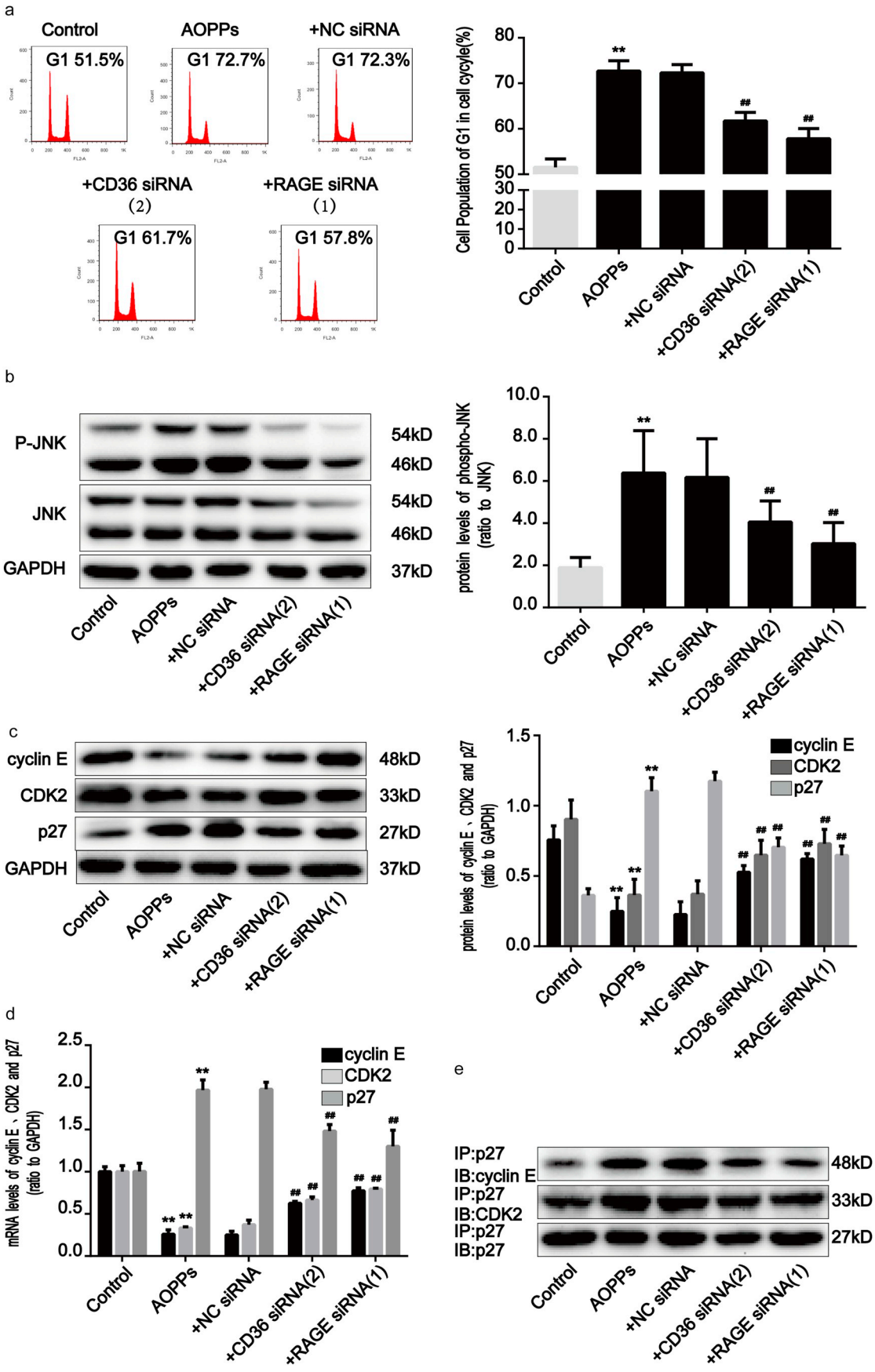

(caption on next page)

Fig. 7. The AOPPs-induced G1 phase arrest in IEC-6 cells was mediated by RAGE and CD36. IEC-6 cells were pre-incubated with RAGE and CD36 siRNA for 48 h before 200 μg/ml of AOPPs treatment for 120min (b) or 24 h (a, c–e). (a) Flow cytometry results showing a decreased percentage of cells in G1 in response to RAGE and CD36 siRNA in AOPPs-treated cells. Quantitative analyses of FACS data represent percentages of G1 phase cells. (b) Expression levels of phosphorylated and total JNK were detected by Western blotting. The AOPPs-induced activation of JNK was inhibited by RAGE and CD36 siRNA. (c) Representative Western blotting and bar graphs depicting densitometry quantification and showing the increase in cyclin E and CDK2 and decrease in p27kip1 resulting from RAGE and CD36 siRNA treatments in AOPPs-treated cells. (d) Bar graphs representing data acquired from qPCR analysis of cyclin E, CDK2 and p27kip1 mRNA expression in AOPPs-treated IEC-6 cells with RAGE and CD36 siRNA treatments. Relative protein and mRNA levels were normalized with GAPDH, respectively. (e) co-immunoprecipitation analysis results showing that both RAGE and CD36 siRNA suppressed AOPPs-induced interaction of p27kip1 with cyclin E-CDK2 complexes. Data are presented as mean ± SD from three independent experiments; error bars indicate SD. *P < 0.05 and **P < 0.01 *versus* control; #P < 0.05 and ##P < 0.01 *versus* AOPPs-treated cells. +CD36 siRNA (2), AOPPs plus CD36 siRNA (2) treatment; +RAGE siRNA (1), AOPPs plus RAGE siRNA (1) treatment.

AOPPs concentrations were expressed as micromoles per liter of chloramine-T equivalents. rAOPPs levels were determined by dividing the AOPPs concentration by albumin levels.

4.3. Isolation of human primary IEC

Surgically resected small intestinal tissue was opened longitudinally, washed in phosphate-buffered saline (PBS), and cut into 5-mm fragments. The intestinal fragments were then resuspended in 10 ml of 5 mM $EDTANa_2$ solution and agitated on a shaking platform for 10 min at 37 °C. Digested samples were then inspected under a microscope to ensure separation of the various tissue components. When > 70% of epithelial crypt/villus units were separated from the intestinal fragments, the digestive solution was neutralized by the addition of 10 ml ice-cold Dulbecco's modified Eagle medium (DMEM) with 10% fetal bovine serum and filtered through a 70 μm filter, followed by centrifugation steps at 1000 rpm for 10 min to remove the supernatant. Finally, cells were washed in PBS and resuspended in ice-cold 70% ethanol prior to flow cytometry analysis.

4.4. Cell cycle analysis

To determine cell cycle distribution, IEC were resuspended in ice-cold 70% ethanol and incubated at 4 °C overnight. The next day, the cells were centrifuged and washed in ice-cold PBS and subsequently incubated with anti-EpCAM (eBioscience™, USA) at 4 °C for 30 min, followed by incubation with 100 μl RNase A at 37 °C for 30 min and 400 μl propidium iodide at 4 °C for 30 min. Cells (1×10^6/ml) were then analyzed using flow cytometry (BD FACSCalubur™, USA) and cell proportions (in %) were measured using FlowJo7.6.1 software.

4.5. Immunohistochemical staining

Paraffin-embedded intestinal tissue sections were cut to a thickness of 4 μm, deparaffinized in xylene, and rehydrated in graded alcohols. Antigen retrieval was achieved by microwaving at 100 °C with an antigen unmasking solution (10 mM citrate buffer, pH 6.0). Hydrogen peroxide (3%) was used to eliminate endogenous peroxidase. After serum blocking, the sections were subsequently incubated with primary antibodies against cyclin E, CDK, RAGE (Abcam), CD36 (Novus), and p27kip1 (Servicebio, Wuhan, China) overnight at 4 °C followed by biotinylated secondary antibodies (Zhongshanjinqiao, Beijing, China). Proteins were visualized as brown pigments via a standard diaminobenzidine (Zhongshanjinqiao) protocol. Slides were then lightly counterstained with hematoxylin and positive immunostaining was examined with an Olympus BX-53 microscope (Olympus).

4.6. AOPPs preparation

AOPPs were prepared *in vitro* by mixing RSA (Sigma, St Louis, MO) with hypochlorous acid (Fluke, Buchs, Switzerland) for 30 min, as described previously [20,21]. AOPPs samples were then dialyzed against PBS for 24 h to remove free HClO and passed through a Detoxi-Gel column (Pierce, Rockford, IL) to remove contaminated endotoxin. The endotoxin levels in AOPPs samples were measured with a Limulus Amoebocyte Lysate kit (BioWhittaker, Walkersville, MD, USA) and were found to be below 0.05 ng/mg protein. The content of AOPPs in the AOPPs treatment and unmodified RSA was 55.05 ± 3.05 μmol/g and 0.2 ± 0.02 μmol/g of protein, respectively.

4.7. Cell culture

The immortalized rat IEC line (IEC-6) was purchased from the Committee on Type Culture Collections (Chinese Academy of Sciences, Beijing, China) and cultured in DMEM supplemented with 10% fetal bovine serum. Cells were maintained at 37 °C in a 5% CO2 atmosphere. For all experiments, cells were grown to 80%–90% confluence and made quiescent by incubation in a serum-free DMEM overnight before stimulation with AOPPs.

4.8. Immunofluorescence

IEC-6 cells were cultured on coverslips, fixed with paraformaldehyde for 15 min, and permeabilized with 0.5% Triton X-100 for 20 min. After blocking with 5% bovine serum albumin for 30 min, the slides were incubated with primary antibodies against cyclin E, CDK2, RAGE (Abcam), p27kip1 (CST), and CD36 (Novus) overnight at 4 °C. Sections were then stained with rhodamine-conjugated secondary antibodies (Invitrogen, Carlsbad, CA) and the nuclei were stained with 4',6-diamidino-2-phenylindole (DAPI). Images were captured using an Olympus BX-53 fluorescence inverted microscope (Olympus, Tokyo, Japan).

4.9. Western blotting analysis

Cultured cells, and frozen intestinal tissue samples from experimental mice, were lysed in RIPA buffer containing 1 × protease cocktail inhibitor (Sigma). Lysates were then separated on SDS-polyacrylamide gels for electrophoresis. The separated proteins were transferred to PVDF membranes (Millipore, Billerica, MA), and the membranes were incubated with primary antibodies overnight at 4 °C. After incubating the membranes with horseradish peroxidase (HRP)-conjugated secondary antibody (Cell Signaling Technology [CST], Beverly, MA, USA) for 1 h at room temperature, immunoreactive proteins were visualized by chemiluminescence detection reagents (Millipore) using the FluorChem E system (ProteinSimple, USA) and blots were quantified using AlphaView SA software (Alpha Innotech Corporation, USA). Several primary antibodies were use. Anti-rabbit cyclin E, anti-rabbit CDK2, anti-rabbit cyclin D1, anti-rabbit cyclin D3, anti-rabbit CDK4, anti-rabbit CDK6, anti-rabbit p27kip1, anti-phospho-rabbit JNK, anti-rabbit JNK, anti-phospho-rabbit ERK1/2, anti-rabbit ERK1/2, anti-phospho-rabbit p38 MAPK, and anti-rabbit p38 MAPK were all purchased from CST. Anti-rabbit RAGE was purchased from Abcam (Cambridge, UK), anti-rabbit CD36 was purchased from Novus (Novus Biologicals, Inc., USA) and anti-mouse GAPDH was purchased from Zhongshanjinqiao (Beijing, China).

4.10. RT-qPCR

Total RNA was prepared from cells using Trizol reagent (Takara,

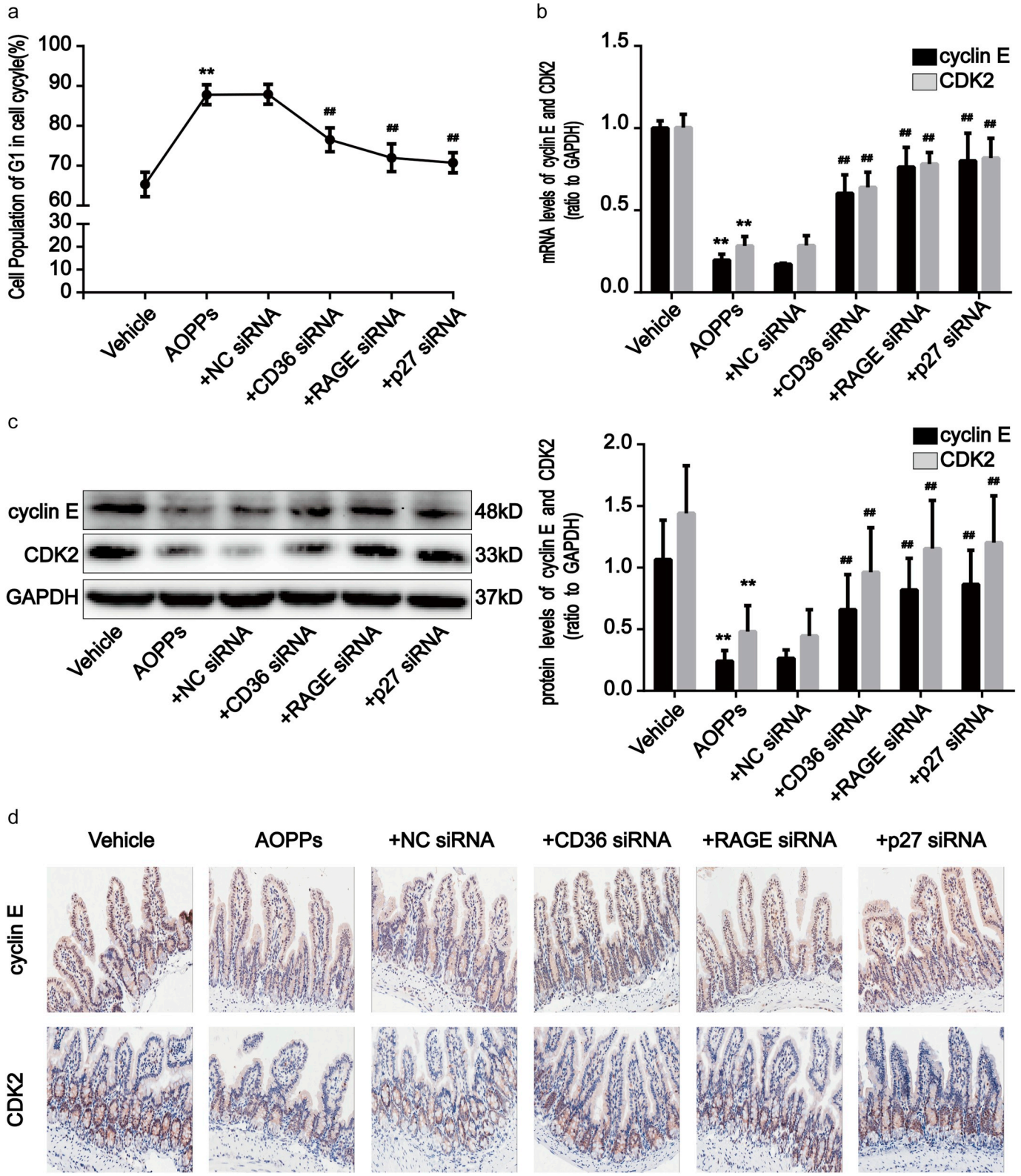

Fig. 8. Acute AOPPs administration induced G1 phase arrest in C57BL/6 mouse IEC. (a) Primary intestinal epithelial cells were collected from mice after treatment with AOPPs for 5 days and analyzed by flow cytometry. The line chart indicates the percentage of G1 phase cells. Data revealed that AOPPs administration induced primary IEC G1 phase arrest compared with mice which were treated with a vehicle, and that treatment with AOPPs + CD36 siRNA, +RAGE siRNA and +p27kip1 siRNA attenuated G1 phase arrest in these cells. (b) Bar graphs representing qPCR analysis showing levels of cyclin E and CDK2 mRNA in mice with or without AOPPs treatment. (c) Representative Western blotting and densitometry quantification showing protein levels of cyclin E and CDK2 in mice with or without AOPPs treatment. Relative mRNA and protein levels were normalized with GAPDH, respectively. (d) Representative images of immunohistochemical staining for cyclin E and CDK2 in mice with or without AOPPs administration. Scale bars, 20 μm. Data are represented as mean ± SD, n = 5; error bars indicate SD. *P < 0.05 and **P < 0.01 *versus* the vehicle group; #P < 0.05 and ##P < 0.01 *versus* the AOPPs-treated group. Vehicle, PBS treatment.

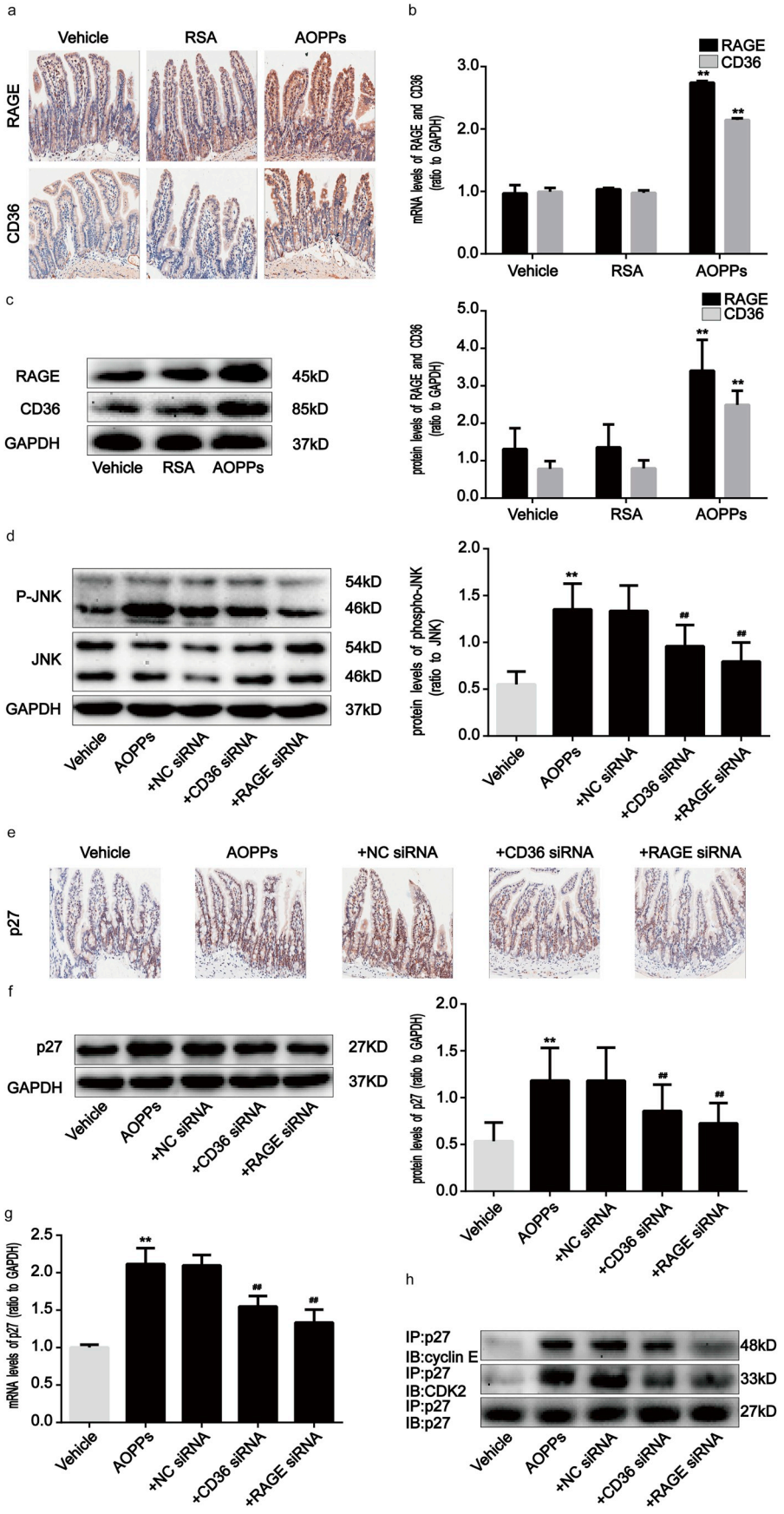

Fig. 9. AOPPs challenge induced the activation of RAGE/CD36, JNK and p27kip1 *in vivo*. (a) Representative images of immunohistochemical staining for RAGE and CD36 in mice with or without AOPPs treatment. Scale bars, 20 μm. (b) Bar graphs representing qPCR analysis showing the levels of RAGE and CD36 mRNA in mice with or without AOPPs administration. (c) Western blotting revealed augmentation of protein expression of RAGE and CD36 in mice with or without AOPPs administration. Relative mRNA and protein levels were normalized with GAPDH, respectively. (d) Representative Western blotting showing significant phosphorylation of JNK in mice IEC after AOPPs treatment. Blockade of RAGE and CD36 significantly reversed the AOPPs-induced activation of JNK. Bar graphs represent densitometric quantification and illustrate the ratio of phosphorylated JNK to total JNK. (e) Representative images of immunohistochemical staining for p27kip1 in mice. Scale bars, 20 μm. (f) Representative Western blotting show protein expression of p27kip1 *in vivo*. (g) Bar graphs representing qPCR analysis showing mRNA levels of p27kip1 *in vivo*. Relative protein and mRNA levels were normalized with GAPDH, respectively. (h) Co-immunoprecipitation analysis showing the interaction of p27kip1 with cyclinE-CDK2 complexes in mice. Data are represented as mean ± SD, n = 5; error bars indicate SD. *P < 0.05 and **P < 0.01 *versus* the vehicle group; #P < 0.05 and ##P < 0.01 *versus* the AOPPs-treated group.

Table 1
Sequences of specific primer pairs.

Primers	5′-3′
CCNE2-Rattus	GCCCAGATAATTCAGGCCAAGA
	CAGACAGTACAGGTGGCCAACAA
CDK2-Rattus	CCTGCACCAGGACCTCAAGAA
	CGGTGAGAATGGCAGAATGCTA
CDKN1B-Rattus and Mus	GAAGATGTCAAACGTGAGAGTGTC
	TCCAAGTCCCGGGTTAGTTC
AGER-Rattus	CTCACAGCCAATGTCCCTAATA
	GAATCAGAGGTTTCCCATCCA
CD36-Rattus	AGGAAAGCCTGTGTACATTTCT
	GTCCTATGCTCATCTTCGTTAGG
GAPDH-Rattus and Mus	GGCACAGTCAAGGCTGAGAATG
	ATGGTGGTGAAGACGCCAGTA
CCNE2-Mus	GTAGACTGGATGGTGCCTTT
	TCTGTCCTCCATGGGTATCT
CDK2-Mus	CAGAGGTGCAGAGAAGGATTAG
	AAGCTGGAAGTCGGGTTAAG
AGER-Mus	CTGGCACTTAGATGGGAAACT
	GCTCTGACCGCAGTGTAAA
CD36-Mus	CCTCTGACATTTGCAGGTCTATC
	GCATTGGCTGGAAGAACAAATC

Table 2
Sequences of specific siRNAs.

siRNA	5′-3′
CDKN1B-Rattus-(1)	CCCGGUCAAUCAUGAAGAATT
	UUCUUCAUGAUUGACCGGGTT
CDKN1B-Rattus-(2)	GGCAUUUGGUGGACCAAAUTT
	AUUUGGUCCACCAAAUGCCTT
CD36-Rattus-(1)	GGAAGUUGUCCUUGAAGAATT
	UUCUUCAAGGACAACUUCCTT
CD36-Rattus-(2)	GGAGCCAUCUUUGAGCCUUTT
	AAGGCUCAAAGAUGGCUCCTT
AGER-Rattus-(1)	CCUUCCAGCUAUCGGAAUUTT
	AAUUCCGAUAGCUGGAAGGTT
AGER-Rattus-(2)	GGAAGCCGGAAAUUGUGAATT
	UUCACAAUUUCCGGCUUCCTT
CD36-Mus	GCUAUUGCGACAUGAUUAATT
	UUAAUCAUGUCGCAAUAGCTT
AGER-Mus	GCUGGCACUUAGAUGGGAATT
	UUCCCAUCUAAGUGCCAGCTT
CDKN1B-Mus	GGCCAACAGAACAGAAGAATT
	UUCUUCUGUUCUGUUGGCCTT
Negative Control- Rattus and Mus	UUCUCCGAACGUGUCACGUTT
	ACGUGACACGUUCGGAGAATT

Table 3
Clinical features of patients with CD (n = 12).

Parameter	CD
Gender	
Male	8
Female	4
Age (years)	33.50 ± 12.72
Albumin (g/L)	33.75 ± 5.38
CRP	29.65 ± 19.86
ESR	29.88 ± 13.01

CD, Crohn's disease; CRP, C reactive protein; ESR, erythrocyte sedimentation rate.

Dalian, China) in accordance with the manufacturer's instructions. First strand cDNA synthesis was carried out by reverse-transcription using PrimeScript™ RT Master Mix (Takara) and qPCR was performed using SYBR Green mix (Takara). Reactions were performed as described previously [20,21] using the LightCycler 480® System (Roche, Basel, Switzerland). The specific sequences of the primer pairs are given in Table 1. The mRNA levels of the genes targeted were determined using the $2^{-\Delta\Delta CT}$ method after normalizing with glyceraldehyde-3-phosphate dehydrogenase (GAPDH).

4.11. Immunoprecipitation

The interaction of p27kip1 with cyclin E-CDK2 or cyclin D-CDK4/6 complexes in cultured IEC-6 cells was evaluated via immunoprecipitation. In brief, cell lysates were pre-incubated with protein A/G agarose beads (7seapharmtech, Shanghai, China) and incubated with the anti-p27kip1 antibody (CST) for 2 h. Protein complexes obtained by immunoprecipitation were then separated using SDS-PAGE gel and detected by Western blotting using anti-cyclin E, anti-CDK2, anti-cyclin D1, anti-cyclin D3, anti-CDK4, anti-CDK6 or anti-p27kip1 rabbit antibodies (CST). The binding of AOPPs to CD36 and RAGE were determined by immunoprecipitation as described above. Immunocomplexes were obtained by incubating cell lysates with anti-CD36 rabbit (Novus) or anti-RAGE rabbit (Abcam) antibodies and assayed separately by immunoblotting with an anti-AOPPs mouse antibody. The anti-AOPPs monoclonal antibody was a gift from Professor Fu Ning (Southern Medical University, Guangzhou, China).

4.12. Cell siRNA transfection

Oligo nucleotide siRNA duplexes were synthesized by Shanghai Gene Pharma (Shanghai, China); the sequences are given in Table 2. Transfections of siRNA into IEC-6 cells were carried out with Lipofectamine 3000 (Invitrogen, Carlsbad, CA) according to the manufacturer's instructions. Approximately 48 h after transfection, cell lysates were collected, and their efficiency was examined by Western blotting.

4.13. Animal experiments

Male C57BL/6 mice (6 weeks, weighing 19–20 g) were obtained from Jinan Pengyue Experimental Animal Breeding Center (Shandong, China) and housed in the Southern Medical University Animal Experiment Center (Guangzhou, China). All mice were randomly divided into eight groups (n = 5 in each group) and given intraperitoneal injections of the following: (i) vehicle group: daily injection of PBS (pH 7.4); (ii) AOPPs group: daily injection of AOPPs (50 mg/kg) for 5 days; (iii/iv/v/vi) AOPPs plus control siRNA/CD36 siRNA/RAGE siRNA/p27kip1 siRNA-treated group: injection of control siRNA, CD36 siRNA, RAGE siRNA or p27kip1 siRNA (all from Gene Pharma) mixed with Entranster™-*in vivo* transfection reagent (Engreen Biosystem, Beijing, China) for 48 h, respectively, before daily injection of AOPPs (50 mg/kg) for 5 days. For each injection, 1 μg/μl of siRNA was mixed with 50 μl Entranster™-*in vivo* following the manufacturer's instructions. Mice were anesthetized and sacrificed after treatment as indicated, and intestinal tissues were collected for various analyses. All animal experiments were approved by the Committee on Animal Experimentation of Southern Medical University. The experimental procedures with animals complied with ARRIVE guidelines and were performed in accordance with the U.K. Animals (Scientific Procedures) Act, 1986. In addition, all animal experiments were approved by the Laboratory Animal Care and Use Committee of Southern Medical University.

4.14. Isolation of mice primary IEC

Mice were killed by cervical dislocation. A midline incision was subsequently made and facilitated removal of the intestines from the duodenum to the ileum. After cleaning the mesentery, the intestines were opened longitudinally, washed in PBS 5 to 6 times, and cut into 5-mm fragments. Tissue was incubated in 2 mM $EDTANa_2$ for 10 min at room temperature to detach the epithelium from the basement membrane. Epithelial cells were then collected by centrifugation at 1000 rpm for 10 min and resuspended in ice-cold 70% ethanol prior to analysis with flow cytometry.

4.15. Statistical analysis

All experimental data are presented as mean ± standard deviation (SD) and experiments were performed in triplicate. Statistical analyses were conducted with SPSS 20.0 software (SPSS, Inc., Chicago, IL). Differences in variables between groups (AOPPs treatment *vs* control, inhibitor treatment, or siRNA treatment) were determined via independent sample t-tests. Pearson correlation and linear regression analysis were applied to assess the correlation between AOPPs levels and cyclin E, CDK, or p27kip1. $p < 0.05$ was considered to be statistically significant.

Conflicts of interest

The authors declare no conflict of interest.

Acknowledgements

This research was supported by the National Natural Science Foundation of China (grants 81500398 and 81470790), Natural Science Foundation of Guangdong Province (2015A030310480 and 2015A030313295) and Guangdong gastrointestinal disease research center (No.2017B02029003).

Appendix A. Supplementary data

Supplementary data to this article can be found online at https://doi.org/10.1016/j.redox.2019.101196.

References

[1] J. Torres, S. Mehandru, J.F. Colombel, L. Peyrin-Biroulet, Crohn's disease, Lancet 389 (2017) 1741–1755.
[2] K.L. VanDussen, A. Stojmirovic, K. Li, T.C. Liu, P.K. Kimes, B.D. Muegge, et al., Abnormal Small Intestinal Epithelial Microvilli in Patients with Crohn's Disease, Gastroenterology, 2018.
[3] R. Okumura, K. Takeda, Maintenance of intestinal homeostasis by mucosal barriers, Inflamm. Regen. 38 (2018) 5.
[4] D. Artis, Epithelial-cell recognition of commensal bacteria and maintenance of immune homeostasis in the gut, Nat. Rev. Immunol. 8 (2008) 411–420.
[5] E.E. Nieuwenhuis, R.S. Blumberg, The role of the epithelial barrier in inflammatory bowel disease, Adv. Exp. Med. Biol. 579 (2006) 108–116.
[6] C. Günther, H. Neumann, M.F. Neurath, C. Becker, Apoptosis, necrosis and necroptosis: cell death regulation in the intestinal epithelium, Gut 62 (2013) 1062–1071.
[7] J.M. Blander, Death in the intestinal epithelium-basic biology and implications for inflammatory bowel disease, FEBS J. 283 (2016) 2720–2730.
[8] X. Escote, M. Zapater, J. Clotet, F. Posas, Hog1 mediates cell-cycle arrest in G1 phase by the dual targeting of Sic1, Nat. Cell Biol. 6 (2004) 997–1002.
[9] D. Fu, D.R. Richardson, Iron chelation and regulation of the cell cycle: 2 mechanisms of posttranscriptional regulation of the universal cyclin-dependent kinase inhibitor p21CIP1/WAF1 by iron depletion, Blood 110 (2007) 752–761.
[10] B.N. Puente, W. Kimura, S.A. Muralidhar, J. Moon, J.F. Amatruda, K.L. Phelps, et al., The oxygen-rich postnatal environment induces cardiomyocyte cell-cycle arrest through DNA damage response, Cell 157 (2014) 565–579.
[11] J.H. Kim, A. Qu, J.K. Reddy, B. Gao, F.J. Gonzalez, Hepatic oxidative stress activates the Gadd45b gene by way of degradation of the transcriptional repressor STAT3, Hepatology 59 (2014) 695–704.
[12] A.J. Valente, T. Yoshida, R.A. Clark, P. Delafontaine, U. Siebenlist, B. Chandrasekar, Advanced oxidation protein products induce cardiomyocyte death via Nox2/Rac1/superoxide-dependent TRAF3IP2/JNK signaling, Free Radic. Biol. Med. 60 (2013) 125–135.
[13] Z.J. Guo, H.X. Niu, F.F. Hou, L. Zhang, N. Fu, R. Nagai, et al., Advanced oxidation protein products activate vascular endothelial cellsvia a RAGE-mediated signaling pathway, Antioxidants Redox Signal. 10 (2008) 1699–1712.
[14] K.F. Peng, X.F. Wu, H.W. Zhao, S. Yan, Advanced oxidation protein products induce monocyte chemoattractant protein-1 expression via p38 mitogen-activated protein kinase activation in rat vascular smooth muscle cells, Chin. Med. J. (Engl) (2006) 1088–1093.
[15] X. Tang, G. Rong, Y. Bu, S. Zhang, M. Zhang, J. Zhang, et al., Advanced oxidation protein products induce hypertrophy and epithelial-to-mesenchymal transition in human proximal tubular cells through induction of endoplasmic reticulum stress, Cell. Physiol. Biochem. 35 (2015) 816–828.
[16] S. Sun, F. Xie, X. Xu, Q. Cai, Q. Zhang, Z. Cui, et al., Advanced oxidation protein products induce S-phase arrest of hepatocytes via the ROS-dependent, β-catenin-CDK2-mediated pathway, Redox Biol. 14 (2018) 338–353.
[17] D.P. McKernan, L.J. Egan, The intestinal epithelial cell cycle, Curr. Opin. Gastroenterol. 31 (2015) 124–129.
[18] M. Hall, S. Bates, G. Peters, Evidence for different modes of action of cyclin-dependent kinase inhibitors: p15 and p16 bind to kinases, p21 and p27 bind to cyclins, Oncogene 11 (1995) 1581–1588.
[19] K. Polyak, J.Y. Kato, M.J. Solomon, C.J. Sherr, J. Massague, J.M. Roberts, A. Koff, p27Kip1, a Cyclin-Cdk Inhibitor, Links Transforming Growth Factor-Beta and Contact Inhibition to Cell Cycle Arrest, Genes and Development, 1994, pp. 9–22.
[20] F. Xie, S. Sun, A. Xu, S. Zheng, M. Xue, P. Wu, et al., Advanced oxidation protein products induce intestine epithelial cell death through a redox-dependent, c-jun N-terminal kinase and poly (ADP-ribose) polymerase-1-mediated pathway, Cell Death Dis. 5 (2014) e1006-e1006.
[21] X. Xu, S. Sun, F. Xie, J. Ma, J. Tang, S. He, et al., Advanced oxidation protein products induce epithelial–mesenchymal transition of intestinal epithelial cellsvia a PKC δ-mediated, redox-dependent signaling pathway, Antioxidants Redox Signal. 27 (2017) 37–56.
[22] P. Wu, F. Xie, M. Xue, X. Xu, S. He, M. Lin, et al., Advanced oxidation protein products decrease the expression of calcium transport channels in small intestinal epithelium via the p44/42 MAPK signaling pathway, Eur. J. Cell Biol. 94 (2015) 190–203.
[23] Y. Son, S. Kim, H.T. Chung, H.O. Pae, Reactive oxygen species in the activation of MAP kinases, Methods Enzymol. (2013) 27–48.
[24] V. Cifarelli, S. Ivanov, Y. Xie, N. Son, B.T. Saunders, T.A. Pietka, et al., CD36 deficiency impairs the small intestinal barrier and induces subclinical inflammation in mice, Cell. Mol. Gastroenterol. Hepatol. 3 (2017) 82–98.
[25] K. Zen, C.X. Chen, Y.T. Chen, R. Wilton, Y. Liu, Receptor for advanced glycation endproducts mediates neutrophil migration across intestinal epithelium, J. Immunol. (2007) 2483–2490.
[26] R. Ciccocioppo, Role of the advanced glycation end products receptor in Crohn's disease inflammation, World J. Gastroenterol. 19 (2013) 8269.
[27] L.L. Zhou, W. Cao, C. Xie, J. Tian, Z. Zhou, Q. Zhou, et al., The receptor of advanced glycation end products plays a central role in advanced oxidation protein products-induced podocyte apoptosis, Kidney Int. 82 (2012) 759–770.
[28] L.L. Zhou, F.F. Hou, G.B. Wang, F. Yang, D. Xie, Y.P. Wang, et al., Accumulation of advanced oxidation protein products induces podocyte apoptosis and deletion through NADPH-dependent mechanisms, Kidney Int. 76 (2009) 1148–1160.
[29] A. Geremia, P. Biancheri, P. Allan, G.R. Corazza, A. Di Sabatino, Innate and adaptive immunity in inflammatory bowel disease, Autoimmun. Rev. 13 (2014) 3–10.
[30] A. Leber, R. Hontecillas, N. Tubau-Juni, V. Zoccoli-Rodriguez, V. Abedi, J. Bassaganya-Riera, NLRX1 modulates immunometabolic mechanisms controlling the host-gut microbiota interactions during inflammatory bowel disease, Front. Immunol. 9 (2018) 363.
[31] E.M. Bradford, S.H. Ryu, A.P. Singh, G. Lee, T. Goretsky, P. Sinh, et al., Epithelial TNF receptor signaling promotes mucosal repair in inflammatory bowel disease, J. Immunol. 199 (2017) 1886–1897.
[32] X. Wang, R. Guo, Y. Lv, R. Fu, The regulatory role of Fos related antigen1 in inflammatory bowel disease, Mol. Med. Rep. 17 (2018) 1979–1985.
[33] R. Pagel, F. Bar, T. Schroder, A. Sunderhauf, A. Kunstner, S.M. Ibrahim, et al., Circadian rhythm disruption impairs tissue homeostasis and exacerbates chronic inflammation in the intestine, FASEB J. 31 (2017) 4707–4719.
[34] S.F. Yan, R. Ramasamy, A.M. Schmidt, The RAGE axis: a fundamental mechanism signaling danger to the vulnerable vasculature, Circ. Res. 106 (2010) 842–853.
[35] W. Cao, J. Xu, Z.M. Zhou, G.B. Wang, F.F. Hou, J. Nie, Advanced oxidation protein products activate intrarenal renin-angiotensin system via a CD36-mediated, redox-dependent pathway, Antioxidants Redox Signal. 18 (2013) 19–35.
[36] M. Gasparitsch, A.K. Arndt, F. Pawlitschek, S. Oberle, U. Keller, M. Kasper, et al., RAGE-mediated interstitial fibrosis in neonatal obstructive nephropathy is independent of NF-kappaB activation, Kidney Int. 84 (2013) 911–919.
[37] Y. Hiraku, F. Guo, N. Ma, T. Yamada, S. Wang, S. Kawanishi, et al., Multi-walled carbon nanotube induces nitrative DNA damage in human lung epithelial cells via HMGB1-RAGE interaction and Toll-like receptor 9 activation, Part. Fibre Toxicol. 13 (2016) 16.
[38] Y. Iwao, K. Nakajou, R. Nagai, K. Kitamura, M. Anraku, T. Maruyama, et al., CD36 is one of important receptors promoting renal tubular injury by advanced oxidation protein products, Am. J. Physiol. Renal. Physiol. 295 (2008) F1871–F1880.
[39] Z. Kabiri, G. Greicius, H. Zaribafzadeh, A. Hemmerich, C.M. Counter, D.M. Virshup, Wnt signaling suppresses MAPK-driven proliferation of intestinal stem cells, J. Clin. Investig. 128 (2018) 3806–3812.
[40] P.R. de Jong, K. Taniguchi, A.R. Harris, S. Bertin, N. Takahashi, J. Duong, et al., ERK5 signalling rescues intestinal epithelial turnover and tumour cell proliferation upon ERK1/2 abrogation, Nat. Commun. 7 (2016) 11551.
[41] Y. Luo, A. Mohsin, C. Xu, Q. Wang, H. Hang, Y. Zhuang, et al., Co-culture with TM4 cells enhances the proliferation and migration of rat adipose-derived mesenchymal stem cells with high stemness, Cytotechnology 70 (2018) 1409–1422.
[42] J. Wen, D. Tan, L. Li, X. Wang, M. Pan, J. Guo, RhoA regulates Schwann cell differentiation through JNK pathway, Exp. Neurol. 308 (2018) 26–34.
[43] L. Zhao, C. Zhang, X. Luo, P. Wang, W. Zhou, S. Zhong, et al., CD36 palmitoylation disrupts free fatty acid metabolism and promotes tissue inflammation in non-alcoholic steatohepatitis, J. Hepatol. 69 (2018) 705–717.
[44] T.W. Lee, Y.H. Kao, T.I. Lee, Y.J. Chen, ADAM10 modulates calcitriol-regulated RAGE in cardiomyocytes, Eur. J. Clin. Investig. 47 (2017) 675–683.
[45] K. Suchal, S. Malik, S.I. Khan, R.K. Malhotra, S.N. Goyal, J. Bhatia, et al., Protective effect of mangiferin on myocardial ischemia-reperfusion injury in streptozotocin-induced diabetic rats: role of AGE-RAGE/MAPK pathways, Sci. Rep. 7 (2017) 42027.

[46] W. Yu, M. Tao, Y. Zhao, X. Hu, M. Wang, 4'-Methoxyresveratrol alleviated AGE-induced inflammation via RAGE-mediated NF-kappaB and NLRP3 inflammasome pathway, Molecules 23 (2018).
[47] C. Bertoli, J.M. Skotheim, R.A. de Bruin, Control of cell cycle transcription during G1 and S phases, Nat. Rev. Mol. Cell Biol. 14 (2013) 518–528.
[48] C.J. Sherr, D-type cyclins, Trends Biochem. Sci. 20 (1995) 187–190.
[49] D.O. Morgan, Principles of CDK regulation, Nature 374 (1995) 131–134.
[50] O. Sangfelt, S. Erickson, J. Castro, T. Heiden, A. Gustafsson, S. Einhorn, et al., Molecular mechanisms underlying interferon-alpha-induced G0/G1 arrest: CKI-mediated regulation of G1 Cdk-complexes and activation of pocket proteins, Oncogene 18 (1999) 2798–2810.
[51] W. Lai, Y. Tang, X.R. Huang, T.P. Ming-Kuen, A. Xu, A.J. Szalai, et al., C-reactive protein promotes acute kidney injury via Smad3-dependent inhibition of CDK2/cyclin, E. Kidney Int. 90 (2016) 610–626.
[52] I. Reynisdottir, K. Polyak, A. Iavarone, J. Massague, Kip/Cip and Ink4 Cdk inhibitors cooperate to induce cell cycle arrest in response to TGF-beta, Genes Dev. 9 (1995) 1831–1845.
[53] C.H. Zhou, M. Xiang, S.Y. He, Z.Y. Qian, Crocetin inhibits cell cycle G1/S transition through suppressing cyclin D1 and elevating p27kip1 in vascular smooth muscle cells, Phytother Res. 24 (2010) 975–981.
[54] A. Ray, M.K. James, S. Larochelle, R.P. Fisher, S.W. Blain, p27Kip1 inhibits cyclin D-cyclin-dependent kinase 4 by two independent modes, Mol. Cell Biol. 29 (2009) 986–999.
[55] L. Marzi, E. Combes, N. Vie, A. Ayrolles-Torro, D. Tosi, D. Desigaud, et al., FOXO3a and the MAPK p38 are activated by cetuximab to induce cell death and inhibit cell proliferation and their expression predicts cetuximab efficacy in colorectal cancer, Br. J. Canc. 115 (2016) 1223–1233.
[56] J. Pucilowska, J. Vithayathil, E.J. Tavares, C. Kelly, J.C. Karlo, G.E. Landreth, The 16p11.2 deletion mouse model of autism exhibits altered cortical progenitor proliferation and brain cytoarchitecture linked to the ERK MAPK pathway, J. Neurosci. 35 (2015) 3190–3200.
[57] A.J. MacNeil, S.C. Jiao, L.A. McEachern, Y.J. Yang, A. Dennis, H. Yu, et al., MAPK kinase 3 is a tumor suppressor with reduced copy number in breast cancer, Cancer Res. 74 (2014) 162–172.
[58] R.A. MacCorkle, T.H. Tan, Mitogen-activated protein kinases in cell-cycle control, Cell Biochem. Biophys. 43 (2005) 451–461.